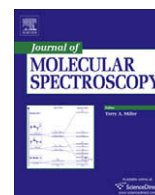




Contents lists available at ScienceDirect

Journal of Molecular Spectroscopy

journal homepage: www.elsevier.com/locate/jmsRotational analysis of the $A^2\Sigma^+_{(v=1,2)} - X^2\Pi_{(v=0)}$ electronic bands of $^{15}\text{N}^{18}\text{O}$ Dmitry Ityaksov^{a,*}, Steven Stolte^{a,1}, Harold Linnartz^{a,b}, Wim Ubachs^a^a Laser Center Vrije Universiteit, De Boelelaan 1081, NL 1081 HV Amsterdam, The Netherlands^b Sackler Laboratory for Astrophysics, Leiden Observatory, University of Leiden, P.O. Box 9513, NL 2300 RA Leiden, The Netherlands

ARTICLE INFO

Article history:

Received 9 February 2009

In revised form 18 March 2009

Available online 2 April 2009

Keywords:

NO spectroscopy

NO isotopologue

Deep-UV spectroscopy

Cavity ring-down spectroscopy

ABSTRACT

Deep-UV spectra of $^{15}\text{N}^{18}\text{O}$ have been recorded using cavity ring-down spectroscopy in the 205–216 nm region. The rotationally resolved spectra have been assigned for a first time as originating from the $v'' = 0$ $X^2\Pi_r$ states toward $v' = 1$ and 2 vibrationally excited levels in the upper $A^2\Sigma^+$ state. Nearly 400 individual line positions have been identified and included in a fit using an effective Hamiltonian method. Accurate ground state values as available from literature were used to derive rovibronic parameters for the $A^2\Sigma^+_{(v=1)}$ and $A^2\Sigma^+_{(v=2)}$ levels. This results in the following values: $T_1 = 46\,427.21(2)\text{ cm}^{-1}$, $B_1 = 1.79635(7)\text{ cm}^{-1}$, $D_1 = 4.14(6) \times 10^{-6}\text{ cm}^{-1}$ and $T_2 = 48\,636.04(2)\text{ cm}^{-1}$, $B_2 = 1.78055(18)\text{ cm}^{-1}$, $D_2 = 5.8(3) \times 10^{-6}\text{ cm}^{-1}$.

© 2009 Elsevier Inc. All rights reserved.

1. Introduction

NO is definitely one of the best studied diatomics in the deep-UV. This has several reasons. The strong NO absorption features that correspond to an excitation of the electronic γ -system ($A^2\Sigma^+ - X^2\Pi_r$) are of atmospheric interest and are used to derive NO column densities in the mesosphere. In addition, NO plays an important role in the atmospheric ozone budget; as a direct reaction product of N_2O oxidation NO contributes both to the tropospheric destruction of ozone and its photochemical formation through smog. Furthermore, NO is one of the major polluting products in combustion and the γ -system is suited for diagnostic tools [1]. Nitric oxide is also interesting from a pure fundamental point of view. Spectroscopic data of NO have been reported over the years by many groups providing a rather complete set of vibronic, rovibrational and pure rotational molecular parameters, for both the main isotopologue $^{14}\text{N}^{16}\text{O}$ [2–14] and several nitric oxide isotopologues $^x\text{N}^y\text{O}$, with $x = 14, 15$ and $y = 16, 17, 18$ [3,6–7,11–12,14–20].

The present work has to be set within the latter context; it focuses on the analysis of so far unreported rovibronic transitions of the heaviest chemically stable NO isotopologue— $^{15}\text{N}^{18}\text{O}$ —in its γ -system. The analysis of the data benefits strongly from previous work for this isotopologue. Accurate $^{15}\text{N}^{18}\text{O}$ ground state values are available from a series of high resolution studies in the submillimeter and infrared [16,19] and rotationally resolved electronic

spectra have been reported in the anode glow of a two-column hollow-cathode discharge tube, yielding rovibronic parameters for the $A^2\Sigma^+_{(v=0)} - X^2\Pi_{r(v=0,1,2,3)}$ bands [12]. In the present work this set of spectroscopic parameters is extended towards wavelengths deeper in the UV-range for excited levels in the upper electronic state: $A^2\Sigma^+_{(v=1,2)} - X^2\Pi_{r(v=0)}$.

2. Experiment

The natural abundance of ^{15}N is about 0.37% and of ^{18}O about 0.20%, i.e. the natural abundance of the $^{15}\text{N}^{18}\text{O}$ is well below 10 ppm. Therefore, the experimental detection of $^{15}\text{N}^{18}\text{O}$ absorptions is based upon a sensitive cavity ring-down detection scheme of an isotopically enriched sample (99% ^{15}N , 95% ^{18}O) that is kept at a stationary pressure of 2 mbar in a 48 cm long cell. Special mirror holders are mounted on opposite sites of the cell for precision alignment of plano-concave mirror sets ($r_{\text{curv}} = 25\text{ cm}$) with a typical reflectivity of $R = 0.995$ and covering the 200–220 nm regime. Tunable laser radiation, generated by frequency-tripling the output of a 10 Hz Nd:YAG pumped dye laser, running near 600 nm (Rhodamine B), is focused into the cell after spatial filtering. The light leaking out of the cavity is recorded by a photo-multiplier tube and subsequently digitized by a 350 MHz oscilloscope. Typical decay times amount to 300 ns and for each frequency value 50 decay events are averaged before a data point is stored. The final bandwidth of the UV-light is about 0.5 cm^{-1} , sufficient to record many of the transitions resolved. However, as the spectrum is rather dense—as will be shown later—this does not prohibit spectral overlaps or blending. An absolute frequency calibration is achieved through a simultaneous I_2 -calibration. The accuracy in the absolute

* Corresponding author. Fax: +31 (0)205987992.

E-mail address: ityaksov@few.vu.nl (D. Ityaksov).¹ Also at: Institute of Atomic and Molecular Physics, Jilin University, Changchun 130012, China.

line position is estimated to be better than 0.1 cm^{-1} . All measurements have been performed at room temperature. Further experimental details are available from Refs. [21–23].

3. Results

The $46\,250\text{--}48\,800\text{ cm}^{-1}$ region has been scanned for transitions of the $(\nu', \nu'') = (1, 0)$ and $(2, 0)$ bands and these are found in the $46\,280\text{--}46\,800$ and $48\,488\text{--}48\,760\text{ cm}^{-1}$ range, respectively.

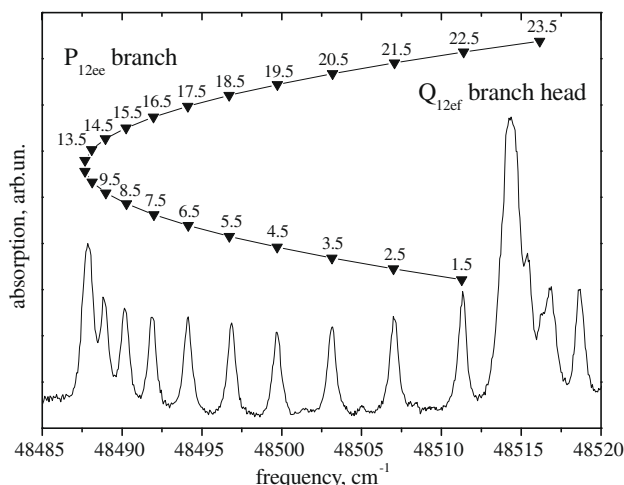


Fig. 1. The P_{12ee} band head region of the $A^2\Sigma^+_{(v=2)} - X^2\Pi_{r(v=0)}$ band.

Referring to [2] and more specifically to [12] where a detailed description of the energy level scheme for the γ -system of NO is given, we expect to observe two sets of rovibronic transitions. These start from the $^2\Pi_{1/2}$ component— R_{21ff} , R_{11ee}/Q_{21fe} , Q_{11ef}/P_{21ff} and P_{11ee} —and the $^2\Pi_{3/2}$ component— R_{22ff} , Q_{22fe}/R_{12ee} , Q_{12ef}/P_{22ff} , P_{12ee} . Here we use the identification of branches as shown in Fig. 2 of Ref. [12]. As the experiment is performed at room temperature both components are populated and the overall spectrum consists of eight resolvable branches. The resolution in the present experiment does not permit to resolve the ρ -doublet components associated with the spin-rotation interaction in the excited state, as was done in Doppler-free excitation studies for the $A^2\Sigma^+_{(v=0)}$ state [24] and the $A^2\Sigma^+_{(v=1)}$ state [25] of the main isotopologue. Fig. 1 shows a scan in the band head region of the P_{12ee} branch for the $A^2\Sigma^+_{(v=2)} - X^2\Pi_{r(v=0)}$ band. This is a relatively clean region of the spectrum where transitions due to other isotopic species are very weak. From the figure it also becomes clear that higher rotational transitions are blended by lower J -values.

The vacuum wavenumbers for all sub-bands are summarized in Tables 1a, 1b and 2a, 2b for the $A^2\Sigma^+_{(v=1)} - X^2\Pi_{r(v=0)}$ and $A^2\Sigma^+_{(v=2)} - X^2\Pi_{r(v=0)}$, respectively. The assignment for transitions starting from $\Omega = 1/2$ and $3/2$ is indicated separately in the tables. In total nearly 400 transitions (from both bands) have been included in a least squares analysis of a $^2\Sigma - ^2\Pi$ transition. For the $^2\Pi$ ground state we have adopted the effective Hamiltonian as described in the analysis of the infrared spectrum by Amiot et al. [7,16]. In the fit we have fixed the molecular constants for the $X^2\Pi$ ground state of $^{15}\text{N}^{18}\text{O}$ ground state constants to accurate values as available from literature. In three papers [12,16,19] consistent and nearly coinciding sets of constants have been published. We have adopted the values derived from the infrared spectrum

Table 1a

List with rovibronic transitions in the $A^2\Sigma^+_{(v=1)} - X^2\Pi_{r(v=0)}$ band for $\Omega = 1/2$. All values are in $[\text{cm}^{-1}]$. An index b indicates that the transition is blended; bh refers to overlapping lines in a bandhead.

J	P_{11ee}		Q_{11ef}/P_{21ff}		R_{11ee}/Q_{21fe}		R_{21ff}	
	Observed	o-c	Observed	o-c	Observed	o-c	Observed	o-c
0.5			46 427.37 ^b	0.17	46 430.95	0.15		
1.5	46 422.57	−0.06	46 426.13 ^{bh}	−0.07	46 433.44	0.04	46 444.17 ^b	0.00
2.5			46 426.13 ^{bh}	0.40	46 436.62	0.08	46 450.77 ^b	−0.12
3.5	46 415.05 ^b	−0.03	46 426.13 ^{bh}	0.32	46 440.48	0.26	46 458.04	−0.11
4.5	46 411.89 ^b	−0.21	46 426.13 ^{bh}	−0.29	46 444.17 ^b	−0.26	46 465.91	−0.04
5.5	46 409.85 ^b	0.18	46 427.37 ^b	−0.20	46 449.20	0.02	46 474.28 ^b	0.00
6.5	46 407.60 ^b	−0.17	46 429.19	−0.06	46 454.46	0.00	46 483.09 ^b	−0.05
7.5	46 406.36 ^b	−0.05	46 431.71 ^b	0.25	46 460.33 ^b	0.05	46 492.55	0.01
8.5	46 405.55 ^{bh}	−0.03	46 434.40	0.19	46 466.71	0.08	46 502.22	−0.25
9.5	46 405.55 ^{bh}	0.27	46 437.54	0.04			46 512.85	−0.09
10.5	46 405.55 ^{bh}	0.03	46 441.62	0.30	46 480.97	0.04	46 524.15 ^b	0.22
11.5	46 406.36 ^b	0.06	46 445.75	0.08	46 488.95	0.08	46 535.57	0.11
12.5	46 407.60 ^b	0.00	46 450.77	0.22	46 497.27	−0.08	46 547.44	−0.07
13.5	46 409.32	−0.12	46 455.91	−0.06	46 506.55	0.19	46 560.01	−0.09
14.5	46 411.89 ^b	0.08	46 461.98	0.06	46 516.02	0.12	46 573.21	0.00
15.5	46 415.05 ^b	0.33	46 468.46	0.07	46 526.16	0.20	46 586.99	0.14
16.5	46 418.16	0.01	46 475.40	0.00	46 536.56	0.00	46 601.04 ^b	0.03
17.5	46 422.13	0.02	46 483.09	0.16			46 615.69	−0.01
18.5			46 491.07	0.07	46 559.33	0.01		
19.5	46 431.71	0.08	46 499.45	−0.14	46 571.48	−0.02	46 646.60	−0.06
20.5			46 508.79	0.09	46 584.16	−0.03	46 662.92	0.00
21.5	46 443.31	0.05	46 518.52	0.17	46 597.60	0.19	46 679.74	0.04
22.5	46 449.85	−0.01	46 528.35	−0.17	46 611.19	0.04	46 696.74	−0.27
23.5	46 457.04 ^b	0.05			46 625.25	−0.17	46 714.75	−0.08
24.5	46 464.65	0.00	46 550.35	−0.08			46 733.05	−0.12
25.5	46 472.63	−0.21					46 751.89	−0.14
26.5	46 481.40	−0.14	46 574.31 ^b	−0.12			46 771.25	−0.16
27.5	46 490.63	−0.15	46 587.67	0.45			46 791.54	0.23
28.5								
29.5	46 510.98 ^b	0.17	46 614.18 ^b	−0.17				
30.5	46 521.45	−0.17	46 628.48	−0.22				
31.5			46 643.58	0.01				

Table 1b

List with rovibronic transitions in the $A^2\Sigma^+_{(v=1)} - X^2\Pi_{(v=0)}$ band for $\Omega = 3/2$. All values are in $[\text{cm}^{-1}]$. An index b indicates that the transition is blended; bh refers to overlapping lines in a bandhead.

J	P_{12ee}		Q_{12ef}/P_{22ff}		R_{12ee}/Q_{22fe}		R_{22ff}	
	Observed	o-c	Observed	o-c	Observed	o-c	Observed	o-c
0.5								
1.5	46 302.37	−0.08	46 306.33 ^{bh}	0.29	46 313.61 ^b	0.38	46 324.02 ^b	0.01
2.5	46 298.18	−0.02	46 305.54 ^{bh}	0.15	46 316.15 ^b	−0.02	46 330.54	0.00
3.5	46 294.40	−0.01	46 305.20 ^b	0.01	46 319.55	−0.01	46 337.61 ^b	0.08
4.5	46 291.05	−0.02	46 305.54 ^{bh}	0.09	46 323.38	−0.03		
5.5	46 288.06	−0.13	46 306.33 ^{bh}	0.16	46 327.66	−0.06	46 352.86	−0.01
6.5	46 285.72	−0.06	46 307.30	−0.04	46 332.37	−0.12	46 361.27	0.05
7.5	46 283.81	−0.01	46 308.94	−0.04	46 337.61	−0.10	46 370.04 ^b	0.00
8.5	46 282.30	−0.02	46 310.99	−0.08	46 343.39	−0.01	46 379.45	0.15
9.5	46 280.97 ^{bh}	−0.31	46 313.67 ^b	0.05	46 349.51	−0.03	46 388.89 ^b	−0.14
10.5	46 280.60 ^{bh}	−0.10	46 316.31 ^b	−0.33			46 399.17	−0.05
11.5	46 280.60 ^{bh}	0.01	46 320.11	0.00	46 363.25	0.05	46 409.85	−0.02
12.5	46 280.97 ^{bh}	0.03	46 324.02	−0.03	46 370.67	−0.06	46 421.05	0.07
13.5	46 281.78	0.03	46 328.40	−0.06	46 378.72	0.00	46 432.52	−0.03
14.5	46 283.07	0.04	46 333.21	−0.11	46 387.17 ^b	0.00		
15.5	46 284.82	0.04	46 338.63	−0.03	46 396.1	0.01	46 457.04	−0.03
16.5	46 286.92	−0.08	46 344.70	0.24	46 405.55	0.08	46 470.07	0.04
17.5	46 289.64	−0.05	46 350.78 ^b	0.05	46 415.05	−0.27	46 483.50	0.05
18.5	46 292.86	0.01	46 357.46	−0.01	46 425.41	−0.23	46 497.52 ^b	0.18
19.5	46 296.58	0.10	46 364.61	−0.07	46 436.62 ^b	0.19	46 511.69	0.00
20.5	46 300.65	0.07	46 372.34	−0.02	46 447.58	−0.10	46 526.49	−0.03
21.5	46 305.20 ^b	0.04	46 380.42	−0.09	46 459.37	−0.04	46 541.78	−0.03
22.5	46 310.17	−0.05	46 388.89 ^b	−0.25	46 471.61	0.00	46 557.52	−0.05
23.5	46 315.90	0.15			46 484.30	0.02	46 573.68	−0.12
24.5	46 321.82	0.05	46 407.60 ^b	−0.23	46 497.52	0.09	46 590.44	−0.07
25.5	46 328.40 ^b	0.14	46 418.00	0.12	46 510.98	−0.08		
26.5	46 335.25	0.02			46 525.03	−0.13	46 625.25	−0.08
27.5	46 342.65	−0.04	46 439.34	−0.10	46 539.73	−0.01	46 643.58	0.12
28.5	46 350.78 ^b	0.15			46 554.57	−0.23		
29.5	46 359.13	0.07						
30.5	46 368.07	0.10	46 475.4	0.01	46 586.27 ^b	−0.08		
31.5	46 377.39	0.01			46 602.78	−0.07		
32.5	46 387.17 ^b	−0.10	46 501.99	0.21				
33.5	46 397.98 ^b	0.33	46 515.89	0.19				
34.5	46 408.48	−0.04	46 529.81	−0.30				
35.5	46 420.00	0.11	46 545.11	0.10				
36.5	46 431.71 ^b	−0.04	46 560.77	0.36				
37.5	46 444.17 ^b	0.07	46 576.03	−0.26				
38.5	46 457.04	0.09	46 592.52	−0.15				
39.5	46 470.31	0.01						
40.5								
41.5	46 498.33	−0.17						

[16], which are considered to give the most accurate representation of the $X^2\Pi_{(v=0)}$ ground state up to high J -levels as probed in the present work. The values used are: $B'_0 = 1.5482463 \text{ cm}^{-1}$, $D'_0 = 4.55190 \times 10^{-6} \text{ cm}^{-1}$, $A'_0 = 123.13895 \text{ cm}^{-1}$, and $A'_{D,0} = 1.5118 \times 10^{-4} \text{ cm}^{-1}$. Although only marginally relevant in the present study we also included A -doubling parameters for the ground state representation: $p'_0 = 1.06 \times 10^{-2}$ and $q'_0 = 7.93 \times 10^{-3} \text{ cm}^{-1}$.

For the $A^2\Sigma^+$ excited state the levels are represented by [25]:

$$E = T_v + B_v[x(x \mp 1)] - D_v[x^2(x \mp 1)^2] - \gamma_v(1 \mp x)$$

with $x \equiv J + 1/2$. We have, in our fitting procedures, used a representation including the last term representing the ρ -doubling, which is inverted in the $A^2\Sigma^+$ state of NO (hence a negative value for γ). We have adopted a value $\gamma'' = -2.64 \times 10^{-3} \text{ cm}^{-1}$, based on results for other isotopologues [13,14,25], but we have verified that adopting $\gamma = 0$ does not influence the outcome on the other molecular constants in our fit. This means that effectively the representation:

$$E = T_2 + BN(N+1) - DN^2(N+1)^2$$

may be used for both the lower ρ -doublet level (F_1 level, or e -level), with $J = N + 1/2$, and the upper ρ -doublet level (F_2 level, or f -level), with $J = N - 1/2$.

The calibrated line positions, as listed in Tables 1a, 1b and 2a, 2b for the observed (2, 0) and (1, 0) bands, were used in the input deck of a weighted least-squares minimization routine, where most of the unblended lines with good signal-to-noise ratio in the (1, 0) band were given an estimated uncertainty of 0.1 cm^{-1} . For the lines in the (2, 0) recorded at somewhat lower signal strength (due to lower CRD mirror reflectivity) a nominal uncertainty of 0.15 cm^{-1} was adopted, although for the best lines also 0.1 cm^{-1} was taken. Blended lines were assigned with larger uncertainties (depending on the amount of blending) and therewith given a lower weight in the fitting routine. The spectral region of the (2, 0) band is covered with additional spectral lines, most likely originating from the (2, 0) band of $^{15}\text{N}^{17}\text{O}$ spectrum; due to this overlap a number of lines are missing in Tables 2a and 2b. In the final round of fitting a total χ^2 of 257 is found for a data set with 380 degrees of freedom (386 lines and 6 parameters). The resulting values for the molecular constants are listed in Table 3. For comparison the molecular constants pertaining to the $A^2\Sigma^+_{(v=0)}$ level in $^{15}\text{N}^{18}\text{O}$ are also listed [12]. Also included in Table 3 are the estimated B -values for the excited state using the standard relation $B_v = B_e - \alpha_e(v + 1/2)$ where the $^{14}\text{N}^{16}\text{O}$ equilibrium values as available from Ref. [12] are used to derive $B_e(^{15}\text{N}^{18}\text{O}) = 1.821157 \text{ cm}^{-1}$ and $\alpha_e(^{15}\text{N}^{18}\text{O}) = 1.631 \times 10^{-2} \text{ cm}^{-1}$. From the table it becomes clear that the values derived here are close to the estimated values.

Table 2a

List with rovibronic transitions in the $A^2\Sigma^+_{(v=2)} - X^2\Pi_{r(v=0)}$ band for $\Omega = 1/2$. All values are in $[\text{cm}^{-1}]$. An index b indicates that the transition is blended; bh refers to overlapping lines in a bandhead.

J	P_{11ee}		P_{21ff}/Q_{11ef}		Q_{21fe}/R_{11ee}		R_{21ff}	
	Observed	o-c	Observed	o-c	Observed	o-c	Observed	o-c
0.5			48 635.72 ^b	−0.31	48 639.95 ^b	0.35		
1.5	48 631.33	−0.13	48 634.81 ^{bh}	−0.19	48 642.51 ^b	0.37		
2.5	48 627.44	0.06	48 634.81 ^{bh}	0.34	48 645.21 ^b	0.02	48 659.44	0.03
3.5	48 623.98	0.17	48 634.81 ^{bh}	0.36	48 648.48 ^b	−0.26	48 666.79 ^b	0.28
4.5	48 620.71	−0.04	48 634.81 ^{bh}	−0.13	48 652.64 ^b	−0.15		
5.5			48 635.72 ^b	−0.20			48 682.26	0.04
6.5	48 615.85 ^b	−0.28	48 637.65 ^b	0.24			48 691.30 ^b	0.47
7.5	48 614.91 ^b	0.34	48 639.95 ^b	0.54	48 668.03	0.06	48 700.05 ^b	0.11
8.5	48 613.33 ^{bh}	−0.19	48 642.54 ^b	0.64	48 673.91	−0.12	48 709.54 ^b	−0.01
9.5	48 613.33 ^{bh}	0.36	48 645.21 ^b	0.31	48 680.62	0.03	48 719.30 ^b	−0.35
10.5	48 613.33 ^{bh}	0.41	48 648.48 ^b	0.09	48 687.64 ^b	−0.01	48 730.14 ^b	−0.12
11.5	48 613.33 ^{bh}	−0.04	48 652.49 ^b	0.10	48 695.26	0.06	48 741.52 ^b	0.16
12.5	48 614.91 ^b	0.59	48 656.94 ^b	0.06	48 703.25	−0.01	48 752.94	−0.01
13.5	48 615.85 ^b	0.08	48 661.68 ^b	−0.19	48 711.68	−0.12		
14.5			48 667.37 ^b	0.01	48 720.48 ^b	−0.37		
15.5	48 620.71 ^b	0.55	48 673.48 ^b	0.14				
16.5	48 622.81 ^b	−0.29	48 679.77	−0.04	48 740.60 ^b	0.20		
17.5	48 626.64	0.11	48 686.84	0.06	48 750.83	−0.09		
18.5	48 630.51	0.06	48 694.17	−0.06	48 761.99	0.07		
19.5			48 701.87 ^b	−0.31				
20.5			48 710.57	−0.04				
21.5			48 719.30 ^b	−0.23				
22.5	48 651.07	0.02	48 728.88 ^b	−0.06				
23.5			48 738.71 ^b	−0.11				
24.5			48 749.16	−0.03				

Table 2b

List with rovibronic transitions in the $A^2\Sigma^+_{(v=2)} - X^2\Pi_{r(v=0)}$ band for $\Omega = 3/2$. All values are in $[\text{cm}^{-1}]$. An index b indicates that the transition is blended; bh refers to overlapping lines in a bandhead.

J	P_{12ee}		Q_{12ef}/P_{22ff}		R_{12ee}/Q_{22fe}		R_{22ff}	
	Observed	o-c	Observed	o-c	Observed	o-c	Observed	o-c
0.5								
1.5	48 511.32 ^b	0.04			48 521.76 ^b	−0.21	48 532.70	0.05
2.5	48 507.04 ^b	0.04	48 514.42 ^{bh}	0.29	48 524.68	−0.13	48 538.79 ^b	−0.27
3.5	48 503.13 ^b	−0.01	48 514.42 ^{bh}	0.59	48 528.11 ^b	0.03	48 545.53 ^b	−0.35
4.5	48 499.71	0.00	48 514.42 ^{bh}	0.45	48 531.68	−0.09	48 553.08	−0.05
5.5	48 496.86 ^b	0.15	48 514.42 ^{bh}	−0.11			48 560.74	−0.07
6.5	48 494.11 ^b	−0.02	48 515.53	0.02	48 540.28	−0.15	48 568.93	0.02
7.5	48 491.90 ^b	−0.08	48 516.68	−0.24	48 545.53 ^b	0.13	48 577.35	−0.08
8.5	48 490.17 ^b	−0.09	48 518.69	−0.07	48 550.80	0.01	48 586.38	0.00
9.5	48 488.90 ^b	−0.06	48 520.98	−0.04	48 556.69	0.08	48 595.93	0.18
10.5			48 523.68	−0.03	48 562.80 ^b	−0.06	48 605.57 ^b	0.02
11.5			48 526.97 ^b	0.14	48 569.44 ^b	−0.09	48 615.85 ^b	0.08
12.5	48 487.85 ^{bh}	0.19	48 530.42	0.04	48 576.54 ^b	−0.09	48 626.64 ^b	0.22
13.5	48 487.85 ^{bh}	−0.23			48 584.19	0.03	48 637.65 ^b	0.16
14.5	48 488.90 ^b	−0.04	48 538.79 ^b	0.02	48 592.10	−0.02		
15.5	48 490.17 ^b	−0.06	48 543.62	0.02	48 600.49	−0.01		
16.5	48 491.90 ^b	−0.05	48 548.77	−0.10	48 609.25	−0.07	48 673.48 ^b	0.22
17.5	48 494.11 ^b	0.01	48 554.67	0.10	48 618.78 ^b	0.22	48 685.95	−0.09
18.5	48 496.86 ^b	0.17	48 560.74	0.04	48 628.29 ^b	0.06	48 699.30	0.05
19.5	48 499.71 ^b	−0.01	48 567.33	0.06			48 712.73 ^b	−0.15
20.5	48 503.13 ^b	−0.05	48 574.41 ^b	0.15			48 726.96	0.02
21.5	48 507.04 ^b	−0.03	48 581.56	−0.14				
22.5	48 511.32	−0.08	48 589.42 ^b	−0.14	48 671.57 ^b	0.35	48 756.71 ^b	0.38
23.5	48 516.20	0.03	48 597.87	0.01	48 683.10	0.05		
24.5	48 521.32 ^b	−0.06	48 606.73	0.14	48 695.26 ^b	−0.05		
25.5	48 526.97 ^b	−0.05	48 615.85 ^b	0.09	48 707.69	−0.30		
26.5			48 625.54 ^b	0.18	48 721.32	0.21		
27.5								
28.5					48 748.49	−0.16		

We note that the findings on the centrifugal distortion constants D for the various vibrational levels are close to each other, but still lacking some consistency. This small deviation may be due to a perturbation in the excited state, which is not accounted

for in our fit, and consequently at this stage the D -constants should be regarded primarily as effective parameters.

In conclusion we have performed a rotational analysis of two bands in the γ -system of the $^{15}\text{N}^{18}\text{O}$ isotopologue yielding for a

Table 3

Molecular parameters for $v=0, 1$ and 2 in the $A^2\Sigma^+$ state of $^{15}\text{N}^{18}\text{O}$. All values are in $[\text{cm}^{-1}]$.

$A^2\Sigma^+$	$v=0^a$	$v=1^b$	$v=2^b$
T	44 130.244 (2)	46 427.21 (2)	48 636.04 (2)
B (observed)	1.812980 (7)	1.79635 (7)	1.78055 (18)
B (estimated)	1.813000	1.796685	1.780370
D (10^6)	4.694 (6)	4.14 (6)	5.8 (3)

^a Taken from Ref. [12].

^b Present work.

first time accurate molecular constants for the $A^2\Sigma^+_{(v=1)}$ and $A^2\Sigma^+_{(v=2)}$ vibrational levels.

Acknowledgments

The authors thank J. Bouma for technical support, and the Netherlands Foundation for Fundamental Research of Matter (FOM) for financial support via their Molecular Atmospheric Physics (MAP) program.

References

- [1] W.G. Bessler, C. Schulz, T. Lee, J.B. Jeffries, R.K. Hanson, Appl. Opt. 42 (2003) 4922–4936.
- [2] G. Herzberg, Molecular Spectra and Molecular Structure. I. Spectra of Diatomic Molecules, Krieger, Malabar, FL, 1991.

- [3] H. Cisak, J. Danielak, M. Rytel, Acta Phys. Pol. A 37 (1970) 67–70.
- [4] R. Engleman Jr., P.E. Rouse, J. Mol. Spectrosc. 37 (1971) 240–251.
- [5] W.L. Meerts, A. Dynamus, J. Mol. Spectrosc. 44 (1972) 320–346.
- [6] R.M. Dale, J.W.C. Johns, A.R.W. McKellar, M. Riggall, J. Mol. Spectrosc. 67 (1977) 440–458.
- [7] C. Amiot, R. Bacis, G. Guelachvili, Can. J. Phys. 56 (1978) 251–265.
- [8] A. Valentin, A. Henry, Ph. Cardinet, M.F. Le Moal, Da Wu Chen, K.N. Rao, J. Mol. Spectrosc. 70 (1978) 9–17.
- [9] A. Henry, M.F. Le Moal, Ph. Cardinet, A. Valentin, J. Mol. Spectrosc. 70 (1978) 18–26.
- [10] C.K.N. Patel, R.J. Kerl, Opt. Commun. 24 (1978) 294–296.
- [11] R. Freedman, R.W. Nicholls, J. Mol. Spectrosc. 83 (1980) 223–227.
- [12] D.X. Wang, C. Haridass, S.P. Reddy, J. Mol. Spectrosc. 175 (1996) 73–84.
- [13] J. Danielak, U. Domin, R. Kepa, M. Rytel, M. Zachwieja, J. Mol. Spectrosc. 181 (1997) 394–402.
- [14] J. Danielak, R. Kepa, M. Zachwieja, J. Phys. B 30 (1997) 4889–4898.
- [15] J.L. Griggs, K.N. Rao, L.H. Jones, R.M. Potter, J. Mol. Spectrosc. 22 (1967) 383–401.
- [16] C. Amiot, G. Guelachvili, J. Mol. Spectrosc. 76 (1979) 86–103.
- [17] J.L. Teffo, A. Henry, Ph. Cardinet, A. Valentin, J. Mol. Spectrosc. 82 (1980) 348–363.
- [18] A.H. Saleck, K.M.T. Yamada, G. Winnewisser, Mol. Phys. 72 (1991) 1135–1148.
- [19] A.H. Saleck, M. Liedtke, A. Dolgner, G. Winnewisser, Z. Naturforsch. 49a (1994) 1111–1118.
- [20] H.P. Liu, Y.Q. Guo, X.Y. Liu, J.L. Lin, F.Y. Li, J.R. Li, Y.Y. Liu, Acta Phys. Sinica 48 (1999) 2030–2037.
- [21] S. Hannemann, E.J. van Duijn, W. Ubachs, J. Mol. Spectrosc. 232 (2005) 151–156.
- [22] D. Ityaksov, H. Linnartz, W. Ubachs, Chem. Phys. Lett. 462 (2008) 31–34.
- [23] D. Ityaksov, H. Linnartz, W. Ubachs, Mol. Phys. 106 (2008) 2471–2479.
- [24] R. Wallenstein, H. Zacharias, Opt. Commun. 25 (1978) 363–367.
- [25] J.E. Murphy, B.A. Bushaw, R.J. Miller, J. Mol. Spectrosc. 159 (1993) 217–229.